

Compatibility test to find a mortar repair for Portland Limestone

Marwa Aly¹ and Sara Pavia²

¹ Dep. of Civil Engineering, Trinity College Dublin, Ireland, 1 email: alym@tcd.ie

² Trinity College Dublin, Ireland, e-mail@xxx.com

Abstract This is part of a more comprehensive investigation which aimed at finding a suitable mortar to repair Portland limestone in historic Irish buildings. Mortars were designed using four binders which included natural hydraulic limes (NHL 2, NHL 3 and NHL5) and hydrated lime (CL90s); siliceous and limestone aggregate in different proportions and several additions (Portland stone dust-PSD-, ground granulated blastfurnace slag –GGBS-, Metakaolin and rice husk ash-RHA). Properties including compressive, flexural and bond strength, open porosity, water absorption, water vapour permeability, capillary suction and bulk density were investigated. According to the results, NHL5 mixes with GGBS and PSD were selected for the compatibility test, which is designed to determine the compatibility and durability of renders. This test was selected based on a preliminary investigation as the mortar would have to be applied as a render to repair the Portland stone weathered and lost over time. The compatibility test includes freeze thaw cycling, adhesion strength and water permeability. It was deemed that this would show clearly which of the compatible mortars had greater adhesion and durability. The compatibility test evidenced that the mortars with 10% PSD and 90% NHL5 reached the higher adhesive strength and water permeability.

1 Introduction

Portland stone is amongst the most common historic building materials used throughout Ireland and the UK, featuring at a significant number of National monuments. In Dublin, most of the important civic and administrative buildings which survive from the 18th century are of Portland stone, including City Hall (1779), the Houses of Parliament (1767), Custom House (1791), the General Post Office (1818), the National Gallery, the National Library and most historic buildings in Trinity College. Portland stone was also extensively used in London,

Manchester, Liverpool, Cardiff, Plymouth, Bristol, Coventry and Oxford. Famous London buildings constructed of Portland stone are the British Museum, Somerset House, the General Post Office, the Bank of England, the Mansion House, the National Gallery, St Paul's Cathedral, Buckingham Palace, the Palace of Westminster and the Tower of London. Portland Stone has also been used across the world and is still used today. Examples include the United Nations headquarters building in New York City, the Casino Kursaal in Belgium and the new BBC Broadcasting House in London which won the 'New Build (non-load-bearing stone) Award' in 2006 (Hughes et al., 2013).

Portland stone is an oolitic limestone of the Jurassic period quarried on the Isle of Portland, Dorset. It has been as highly favoured as a monumental and architectural material over time as it is strong and well cemented without being too stiff and brittle, so that it can be readily cut and carved. Geologically, the Portland beds are divided into three major types, namely the lower Portland Sand, the middle Cherty Limestone series and the upper Freestone Limestone series (Arkell, 1933). Commercially, the Portland Stone consists of three main units named Whitbed, Roachbed and Basebed (Fig. 1). The Roach-bed is a tough grey-brown oolitic limestone riddled with casts of shells. The Whit-bed is a buff-coloured oolitic limestone with a large quantity of comminuted shells. The Base-bed was used in the building subject to study. It is a soft, white oolitic limestone of fine texture and uniform colour with rare shells. Bedding planes are generally absent, and the stone is 'free,' i.e. may be worked in any direction.

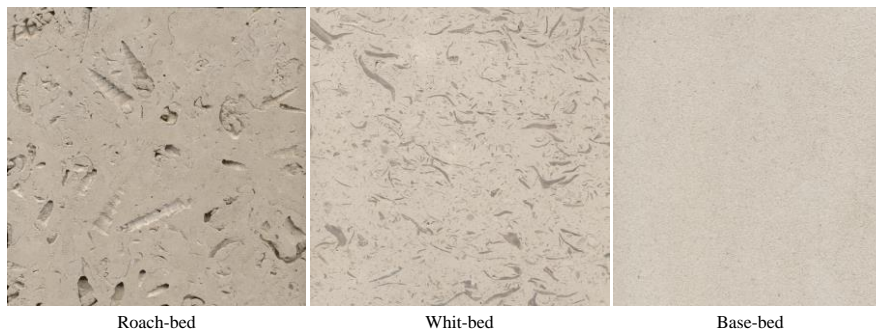


Fig. 1 Portland stone beds (Dawson Stone 2015).

Many different repairs have been applied to Portland stone throughout history; some have fulfilled their protective role and eventually weathered over time while others have been detrimental to the substrate. There is a lack of precise and systematic data on the composition, properties and behaviour of these repairs. This paper is part of a more comprehensive investigation which intended to fulfil this gap and find a suitable mortar to repair Portland limestone in historic Irish buildings.

The investigation was divided into three stages (Fig. 2). The first stage was designed to select the binder, aggregate type and proportions of the repair mortar. Mortars were produced with four binders including CL90s, NHL2, 3.5 and 5, two types of aggregate namely Portland stone aggregate and siliceous sand and three binder/aggregate ratios. Furthermore, a commercial mix commonly used to repair Portland and other monumental stones was studied.

No significant differences were found in the properties of mortars made with Portland stone aggregate and siliceous sand (Aly and Pavía, 2016). It was also noted that the porosity, water absorption, suction and water vapour permeability of the commercial mix were 60, 66, 68 and 59% lower respectively than those of Portland stone. In addition, the 1:3 (binder/aggregate) NHL5 mortar showed the closest hygric properties to the Portland stone, the highest bond strength and remarkable mechanical properties. Based on these results, the 1:3 NHL 5 siliceous sand mortar mixed to flow 165 ± 5 mm was selected for further testing.

The aim of the second stage was to improve bond strength and durability by using additives. Four additives namely Portland stone dust (PSD), ground granulated blastfurnace slag (GGBS), Metakaolin (MK), and rice husk ash (RHA) were investigated at three levels of lime replacement (10, 20 and 30%). Approximately 700 samples were tested at 28, 90, 180 days. The second stage evidenced that the NHL5/20%GGBS and NHL5/10%PSD mixes had the greatest bond strength and closest mechanical and hygric properties to those of the stone (Aly and Pavía, 2015). Therefore, they were selected for the compatibility test (third stage).

This paper presents the results of the compatibility test which is designed to assess the quality of renders. The assessment is based on the adhesion strength and water permeability of the hardened render applied on a specific substrate, following exposure to freezing/heating cycles.



Fig. 2 Stages of investigation.

2 Materials and Method

2.1 Materials

Natural hydraulic lime NHL 5 complying with EN 459-1 was used as a binder (Table 1). The NHL5 binder used contains some available (free) lime $\text{Ca}(\text{OH})_2$

(15-20% after slaking) and a significant amount of clinkers similar to those found in Portland cement (mainly belite C_2S -Table 1), and has no impurities relevant to classification and labelling and a minimal presence of Al_2O_3 , sulphates and alkalis (very low in the parent limestone).

Table 1 Mineral composition of NHL 5 in % (St Astier/CESA 2015). Insoluble 5.6%.

$Ca(OH)_2$	$CaCO_3$	C_2S	C_3A	C_2AS	C_4AF	$CaSO_4$
22	23	43	0.7	1.3	0.7	0.7

Siliceous aggregate (pure quartz sand) with grading similar to that of the CEN normal sand was used. The chemical composition and amorphousness of the GGBS are presented in Table 2. The chemical composition was assessed by XRF using a Quant'X EDX Spectrometer and UniQuant analysis package. The amorphousness was evidenced with X-ray diffraction (XRD), using a Phillips PW1720 XRD with a PW1050/80 goniometer and a PW3313/20 Cu ka anode tube at 40 kV and 20 mA (Walker et al. 2014).

Table 2 Chemical composition and amorphousness of GGBS (Walker et al. 2014).

SiO_2	Al_2O_3	CaO	FeO_3	SO_3	MgO	Rate of amorphousness
34.14%	13.85	39.27	0.41	2.43	8.63	Totally

Portland stone dust (PSD) was obtained by grinding Portland stone aggregate. The PSD consists mainly of calcite ($CaCO_3$), with traces of silica in the form of quartz (SiO_2). The particle size distribution of the dust is included in figure 3. Base-bed Portland stone slabs (400x400x40 mm) quarried in the UK were used for the compatibility test. The mechanical and hygric properties of the stone as reported by the supplier and tested in our laboratories are included in Table 3.

Table 3 Mechanical and hygric properties of Portland stone basebed. COV (%) in brackets.

	Provided by supplier	Measured in the laboratory
Compressive (MPa)	41.15	54.23 (1.76)
Flexural (MPa)	6.85	6.23 (1.12)
Porosity (%)	18.81	15.4 (0.6)
Water absorption (%)	8.86	7.19 (0.79)
Suction ($gm/m^2 \cdot sec^{0.5}$)	NA	82.16 (2.54)
Vapour Permeability ($kg/m \cdot s \cdot Pa$)	NA	2.75×10^{-11} (7.83)
Bulk density (Kg/m^3)	NA	2159.15 (0.6)

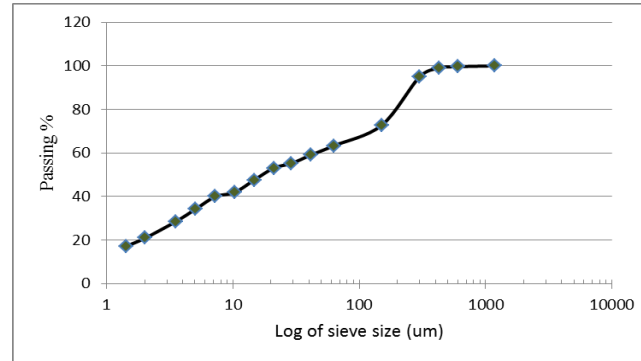


Fig. 3 Particle size distribution of Portland stone dust.

2.2 Mixing and curing

The lime, additives and aggregate were dry mixed for 2 min. Water was added to achieve a 165 ± 5 mm initial flow diameter and mixed for 2 min at low speed and finally at high speed for 1 min. A 10mm thick mortar coat was applied on the Portland stone slabs ($400 \times 400 \times 40$ mm) (Fig. 6). The slabs were then covered with damp hessian and kept for 28 days at $20 \pm 2^\circ\text{C}$ temperature. The mortar were cured and stored according to EN 459-2.

Table 4. Composition and water content of the mortars investigated

Mix	Binder/additions			Binder/sand (by weight)	Water/binder
	NHL5	GGBS	Portland stone dust		
Control	100%	0	0	1:1	0.73
20%GGBS	80%	20%	0	1:1	0.68
10%PSD	90%	0	10%	1:1	0.69



Fig. 4 Portland stone slabs rendered with 10 mm mortars in table 4.

2.3 Methods

Physical and mechanical properties of the mortars. The properties measured were compressive (EN 1015-11:1999), flexural strength (EN 1015-11:1999), water retention (EN 459-2: 2010), water absorption, porosity (RILEM 1980), bulk density (RILEM 1980), capillary suction (EN 1925) and vapour permeability (EN 1015-19). The mortar bond strength was measured in stone-mortar specimens using pull-out tests (Fig. 5) as described in (Maravelaki-Kalaitzaki et al., 2013). This test is designed to measure the direct tensile strength of the interface rather than the shear strength of the interface in conventional pull off tests. In order to avoid shear force, a hole was drilled in the stone pieces sandwiching the mortar and the sample pulled apart through pins inserted in the holes, Figure 5. The results reported are the arithmetic mean of 3-6 tests with their coefficients of variation.



Fig. 5 Set up of pull-out test to measure bond strength between Portland stone and mortar.

Compatibility test. The compatibility (of one-coat rendering mortars with substrate) test was performed according to EN1015-21:2002. The cured slabs rendered with mortars were subjected to two series of thermal-freezing and humidification-freezing respectively of four cycles each. In the thermal/freezing cycles, the sample surface is first subject to infrared heating at a temperature of $60\text{ }^{\circ}\text{C} \pm 2\text{ }^{\circ}\text{C}$ maintained for 8h and 15min and later stored in a deep freeze at $-15\text{ }^{\circ}\text{C} \pm 10\text{ }^{\circ}\text{C}$ air temperature for 15h and 15 min. In the humidification-freezing cycles, the slabs are first partially immersed in water to a depth of c.5 mm, for 8h and 15 min and then subjected to freezing as above. Between cycles, the slabs were stored in standard conditions at $20\text{ }^{\circ}\text{C} \pm 2\text{ }^{\circ}\text{C}$ and $65\pm 5\text{ \% RH}$.

Following cycling, the slabs endured the permeability and the adhesive strength test. In the permeability test (Fig. 6), a metal cone was bonded to the rendered surface using silicone and allowed to set for one day. Then a permanent head of 100 mm of water was maintained on the render surface and the quantity of water (ml) required to keep this level constant over a 48 h period recorded. After the permeability test, five cores (of 63 mm diameter) were drilled from the slabs and subjected to the adhesive test (Fig.7) according to EN 1015-12.

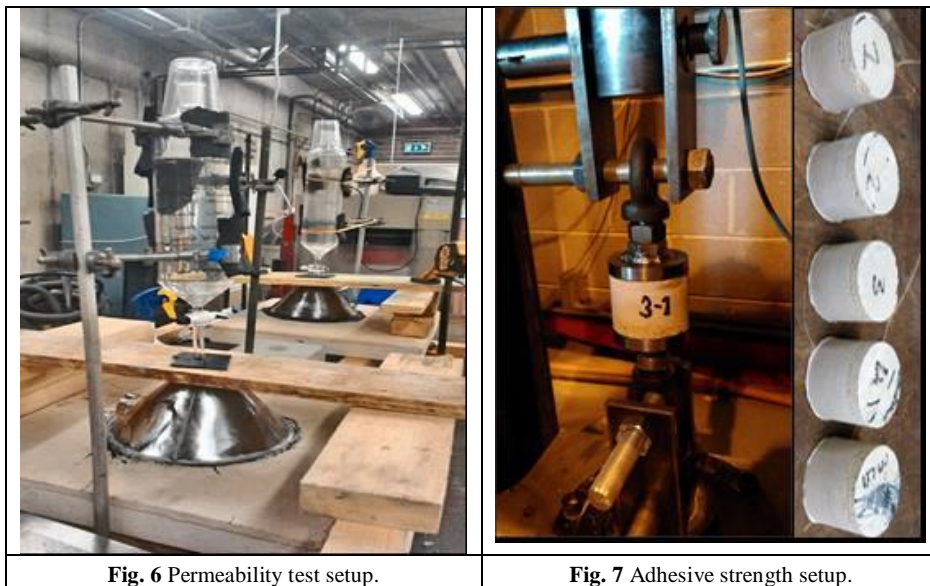


Fig. 6 Permeability test setup.

Fig. 7 Adhesive strength setup.

3 Results and discussion

3.1 Mechanical and hygric properties of NHL5 mortars

The mechanical properties of the repair mortars are lower therefore compatible with the Portland stone (Table 5). The 10% PSD replacement enhanced the compressive strength of the NHL5 mortar at 28 and 90 days (by 56 and 17 % respectively-Table 3) however, at 180 days, the strength slightly lowers by 3 %. The 10% PSD replacement didn't significantly affect the flexural strength of the NHL5 mortar however it nearly doubles its bond strength.

Menéndez et al. 2003 and Tsvilis, S., et al. 1999 reported up to 10% limestone powder replacing Portland cement without impairing the 28-day compressive strength.

The replacement of NHL5 with 20%GGBS, significantly improves the compressive strength of NHL5 mortars at all ages (it doubles the strength at 28 days and increases by over 30% ultimate strengths at later ages). It slightly improved the flexural strength of the NHL5 mortar and increased its bond strength by 27%. This was expected as GGBS is a latent hydraulic binder that becomes activated forming hydrates.

Table 5 Mechanical properties of the NHL5 mortars at 1,7,28, 90 and 180 days. COVs (%) in brackets.

Mortar	Compressive strength (MPa)					Flexural strength (MPa)				Bond s. (MPa) 28 days
	1	7	28	90	180	1	28	90	180	
100%NHL5	0.92 (10.0)	5.01 (9.4)	9.53 (1.7)	18.21 (13.4)	20.49 (4.2)	0.06 (0.01)	0.92 (3.2)	2.02 (6.8)	1.72 (4.0)	0.26
20%GGBS	1.10 (0.1)	8.82 (11.3)	20.58 (5.0)	30.43 (6.6)	30.68 (3.1)	0.08 (3.8)	1.70 (4.7)	2.24 (14.0)	2.23 (1.1)	0.33
10%PSD	0.93 (8.2)	4.69 (3.5)	14.89 (15.1)	21.33 (8.6)	19.85 (6.7)	0.07 (12.0)	1.34 (5.8)	2.05 (4.4)	1.73 (3.9)	0.40

The hygric properties of the mortars are included in Table 6. The 20%GGBS replacement significantly increases the NHL5 mortar's bulk density and notably lowers its porosity, water absorption and capillary suction (36-65%) while the 10%PSD replacement increases density to some extent lowering porosity (by 8%), water absorption (-9%) and capillary suction (-30%). The severe reduction in hygric properties by the GGBS poses a threat with regard to compatibility (Pavía and Bolton 2000).

Table 6 Hygric properties of NHL5 mortars at 90 days and Portland Limestone. COVs ranging from 0.08 and 7.9% (c. 90% of results show COVs under 5%). In brackets % reduction with respect to control mortar NHL5.

	Porosity (%)	Water absorption (%)	Bulk density (Kg/m ³)	Suction (gm/m ² .sec ^{0.5})	Vapour Perm*10 ⁻¹¹ (kg/m·s·Pa)
100%NHL5	21.8	11.6	1874.7	141.5	2.7
20%GGBS	13.8 (-36%)	7.04 (-39%)	1914.3	49.0 (-65%)	2.4 (-10%)
10%PSD	20.0 (-8%)	10.5 (-9%)	1890.9	99.0 (-30%)	2.1 (-20%)
Portland stone	15.4	7.2	2159.1	82.1	2.7

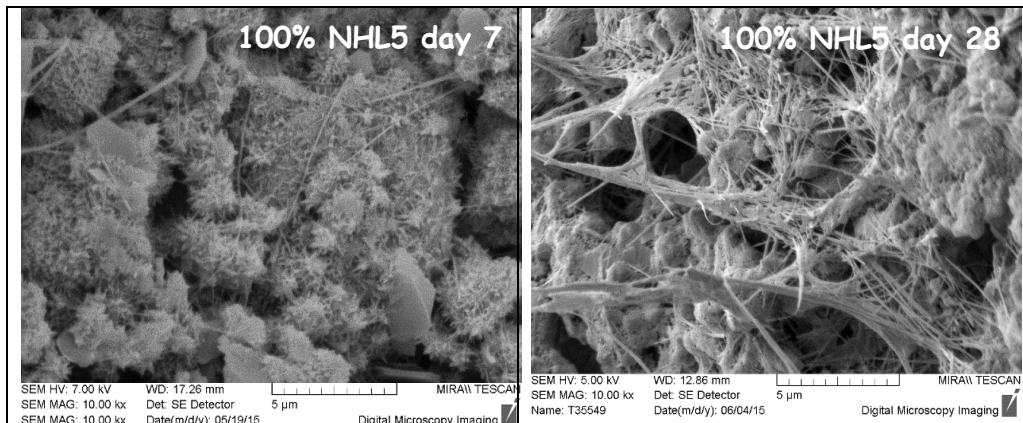
It was also noted that despite the additions, the NHL5 mortars remain permeable to water vapour, with values very close to the Portland stone, as the GGBS and limestone dust only lowered the vapour permeability of the NHL5 mortar by 10 and 20% respectively.

GGBS is more efficient at lowering suction than the stone dust (65% drop vs 30%) which is attributed to the presence of more cementitious hydrates refining the pore structure and blocking the NHL5 mortar capillary-active pores.

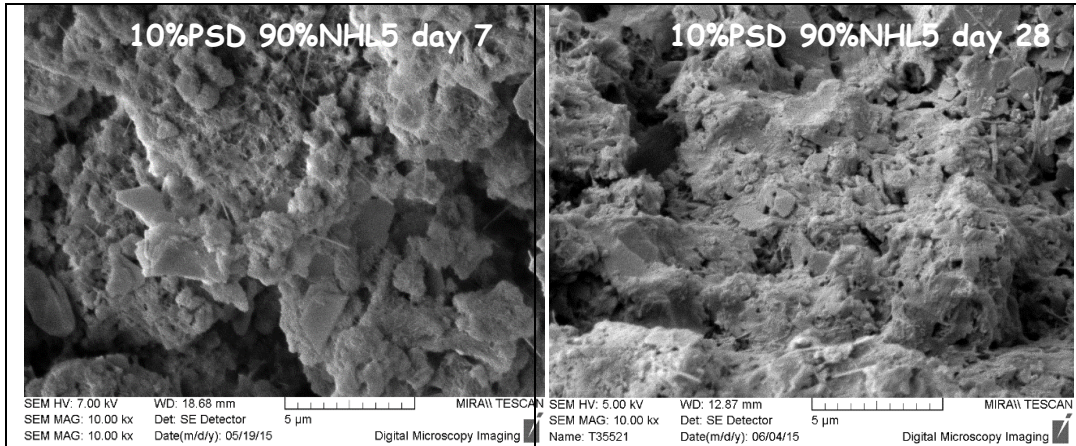
The porosities of the NHL5 and NHL5/10%PSD mortars are similar and comparable to the 18-40% values documented by Moropoulou et al. (2004) for hydraulic lime mortars in ancient Mediterranean structures, and greater than the porosity of the Portland stone (Table 4). The porosity of the NHL5 mortar (21.85%) agrees with results by Silva et al. (2015) who recorded 23% values for 1:4.5, NHL5/aggregate mortars aged 3 years. It also agrees with Gulotta et al. (2013) who reported c.21% values for NHL5 mortar, with standard quartz sand at B/A ratio of 1:3 by weight. Furthermore, it is consistent with the 24% values in Cosgrove and Pavía (2009) (1:3 by weight, NHL5 mortar made to flow 175 mm).

3.2 Microstructure of NHL5 mortars

The Portland limestone dust dramatically changes the microstructure of the NHL5 mortar making it denser by producing different hydrates and more abundant carbonated lime- CaCO_3 - when compared to the NHL5 mortar (Figs 8-11). In Portland cement, limestone dust provides ample carbonate ions to participate in hydration reactions that lead to enhanced aluminate reactivity, stabilization of ettringite and the formation of more voluminous and potentially stiffer carboaluminates in place of sulfoaluminates (Bentz et al. 2015). The NHL5 contains little aluminates (Table 1) however, it is obvious from the SEM analysis that the limestone dust has changed the nature of the hydrates (Figs 9 and 11).

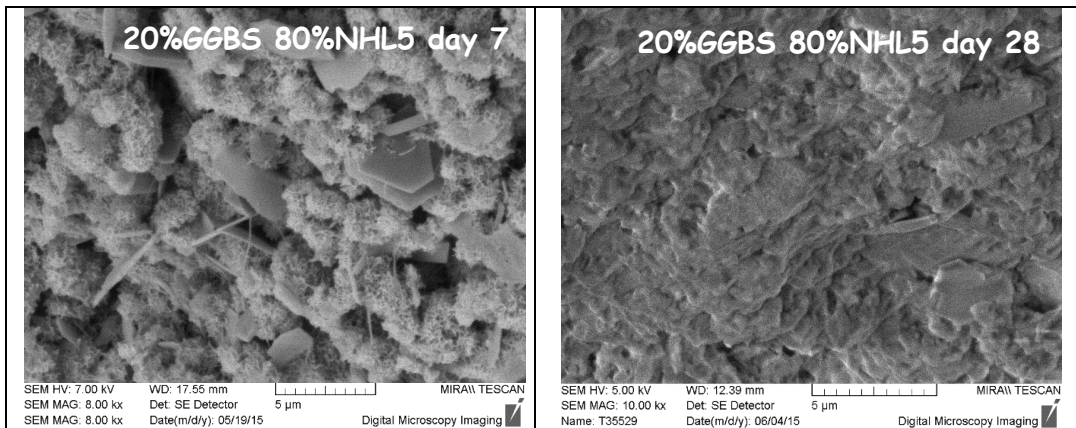


Figs 8 and 9. Microstructure of the NHL5 (control) mortar showing abundant clusters of needle-shaped hydrates (probably CSH) and occasional hexagonal portlandite ($\text{Ca}(\text{OH})_2$) plates at 7 days; turning into a continuous network of fibrous hydrates that join particles of carbonated lime (CaCO_3) at 28 days.



Figs 10 and 11. Microstructure of the Portland stone dust mortar at 7 days (left) and 28 days (right). The Portland limestone dust dramatically changes the microstructure of the NHL5 mortar making it denser and producing different hydrates and more abundant carbonated lime- CaCO_3 - totally covering the dust and aggregate.

The microstructure of the NHL5 mortar with GGBS at 7 days is similar to the NHL5 (control) mortar, displaying abundant clusters of needle-shaped hydrates (probably CSH) and occasional hexagonal portlandite ($\text{Ca}(\text{OH})_2$) plates however, at 28 days the density of the GGBS mortar is significantly greater with more cementing hydrates and little pores.



Figs 12 and 13. Microstructure of the NHL5 mortar with GGBS at 7 days (left) and 28 days (right). At 7 days the microstructure is similar to the NHL5 (control) mortar with abundant clusters of needle-shaped hydrates (probably CSH) and occasional hexagonal portlandite ($\text{Ca}(\text{OH})_2$) plates however, at 28 days the density is greater with little pores.

3.3 *Compatibility test*

The Portland stone dust greatly improves the adhesion of the NHL5 mortar to the Portland limestone substrate (more than doubles it)-Figure 14. This agrees with the SEM analysis which evidenced CaCO_3 and hydrates completely covering the dust and the aggregate thus providing internal cohesion to the material. The drastic change in the nature of hydrates brought about by the Portland stone dust (Figures 8-11) may have also contributed to the enhanced bond.

The enhanced cohesion provided by the limestone dust can be related to the high water absorption of the dust (suction $82.16 \text{ gm/m}^2.\text{sec}^{0.5}$ -Table 3) helping achieve a greater bond. Groot 1993, studying mortar-brick bond, states that moisture and material transfer at the interface are needed to develop bond, as bond is determined by the binder nature at the interface. The high water absorption of the dust is probably enhancing the precipitation of carbonated lime binder and cementing hydrates at the interface, and these enhance the strength of the bond. A close phenomenon has been noted in lime mortars including limestone aggregate by Scannell et al. (2014) and Pavía and Aly (2016) and Aly and Pavía (2016).

In addition, the enhanced cohesion provided by the limestone dust may be attributed to the dust acting as a nucleation sites that enhance the formation of CaCO_3 crystals in the binder. This was similarly reported for limestone sand in PC matrices (Péra et al. 1999) and calcitic aggregates in hydrated lime mortars (Lanas and Alvarez, 2004). As noted by Péra et al. 1999; Bonavetti et al. 2001; Menéndez et al. 2003; Ye et al. 2007; Weerdt et al., 2011, Bentz et al., 2015, Siad et al. 2015, in Portland cement matrices, limestone dust accelerates and amplifies the silicate reactions by providing additional nucleation points for calcium hydroxide crystals at early hydration ages, accelerating clinker hydration and increasing early strength.

The Portland stone dust also increased the water permeability of the NHL5 mortar by c. 40% (Figure 15). This can be partly attributed to the high porosity, water absorption and suction of the Portland stone dust (18.81%, 7.19% and $82.16 \text{ gm/m}^2.\text{sec}^{0.5}$ respectively).

The NHL5 mortar with 20%GGBS shows c.50% decrease in adhesive strength compared to control mortar. This mortar showed the highest mechanical strength at all ages therefore the lower adhesion can be due to weathering during cycling or testing inconsistencies e.g when drilling the cores.

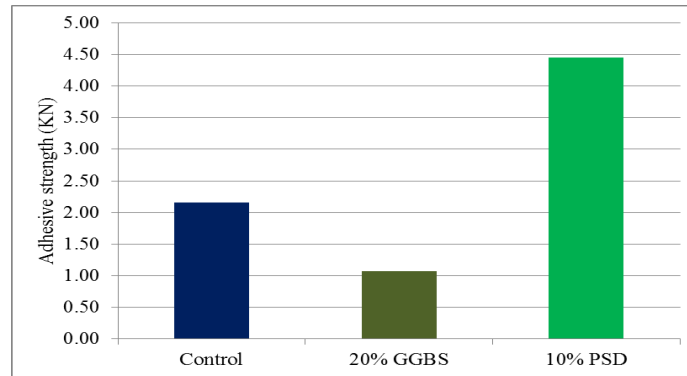


Fig. 16 Adhesive strength according to EN 1015-12.

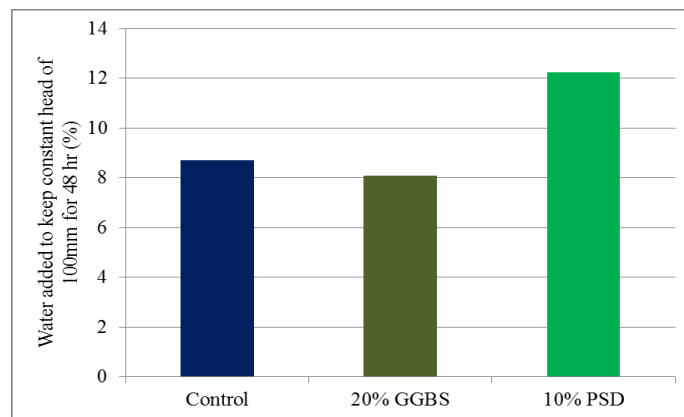


Fig. 15 Permeability to a permanent head of water.

4 Conclusion

The mechanical properties of the NHL5 repair mortars are lower therefore compatible with the Portland limestone however, the severe reduction in hygric properties recorded in the NHL5 with 20% GGBS replacement may pose a threat with regard to compatibility. The exposure to freezing/heating cycles in the compatibility test does not seem to undermine the adhesive strength and durability of the mortars.

It is concluded that the best mortar repair is the NHL5 with 10% Portland stone dust which more than doubles the adhesion of the NHL5 mortar to the Portland limestone substrate. The drastic change in the nature of hydrates and the complete coverage by carbonated lime and hydrates brought about by the Portland stone

dust have probably contributed to the enhanced bond. In addition, the dust acting as a nucleation sites that enhance the formation of CaCO_3 binder has probably enhanced adhesion. The enhanced bond provided by the limestone dust can also be related to the high water absorption of the limestone dust boosting the precipitation of carbonated lime binder and cementing hydrates at the interfaces.

Acknowledgment

The authors wish to thank the Irish Research Council for funding this research. We also thank the Office of Public Works for funding the project and Mr. John Cahill for facilitating investigation and site work. The testing was carried out in the Department of Civil, Structural and Environmental Engineering, Trinity College Dublin. The authors thank Chief Technician Dr Kevin Ryan, for facilitating our laboratory work, Mr. Eoin Dunne for doing the sieve analysis and sedimentation test for Portland stone dust, Dr. Michael Grimes and Mr. Dave McAuley for their assistance with testing and Dr. Gerard Joseph McGranaghan for assistance in setting up the controlled infra-red heating system.

5 References

Hughes, T., Lott, G. K., Poultney, M. J., & Cooper, B. J. (2013). Portland Stone: A nomination for " Global Heritage Stone Resource" from the United Kingdom. *Episodes*, 36 (3), 221-226.

Pavía S. and Bolton J., *Stone, Brick and Mortar*. Wordwell Bray, Co Wicklow. 2000.

Arkell, W.J. *The Jurassic system in great Britain*, Oxford - Clarendon Press. 1933.

Dawson Stone (2015) www.dawsonstonemasonry.co.uk/materials.

Maravelaki-Kalaitzaki, P. et al. (2013) Physico-chemical and mechanical characterization of hydraulic mortars containing nano-titania for restoration applications. *Cement and Concrete Composites*. 36: p. 33-41.

EN 459-1 (2010). *Building lime. Part 1: Definitions, specifications and conforming criteria*. European Committee for Standardisation CEN, Brussels.

EN 459-2 (2001). *Building lime. Test methods*.

EN 1015-11 (1999). *Methods of test for mortar for masonry. Determination of flexural and compressive strength of hardened mortar*.

EN 1925 (1999). Natural stone test methods. Determination of water absorption coefficient by capillarity.

RILEM (1980). Recommended tests to measure the deterioration of stone and assess the effectiveness of treatment methods. *Materials and Structures* 13: 175–253.

Tsivilis, S. et al. (1999) A study on the parameters affecting the properties of Portland limestone cements. *Cement and concrete composites*. 21(2): p. 107-116.

Moropoulou, A., Bakolas A. et al. (2005). Composite materials in ancient structures. *Cement and Concrete Composites* (27): 295–300.

Silva, B. A., Pinto, A. F. and Gomes, A. (2015). Natural hydraulic lime versus cement for blended lime mortars for restoration works. *Construction and Building Materials*, 94, 346-360.

Saint Astier/CESA (2015) Natural Hydraulic Limes (NHL) Technical data sheet. Conforming to European Regulations (CE) n° 1907/2006. NHL 5.
<http://www.stastier.co.uk/nhl/health-safety/nhl5-hs.htm>

Gulotta, D., S. Goidanich, et al. (2013). Commercial NHL-containing mortars for the preservation of historical architecture. Part 1: Compositional and mechanical characterisation. *Construction and Building Materials* 38(0): 31-42.

Cosgrove, K. and Pavía, S. (2009). Mechanical and Fluid Transfer Properties of some Lime and Portland Cement Mortars. In PROHITEC 2009 International Conference (pp. 1603-1607).

Siad, H., Alyousif, A., Keskin, O. K., Keskin, S. B., Lachemi, M., Sahmaran, M., & Hossain, K. M. A. (2015). Influence of limestone powder on mechanical, physical and self-healing behavior of Engineered Cementitious Composites. *Construction and Building Materials*, 99, 1-10.

De Weerd, K., et al. (2011) Synergy between fly ash and limestone powder in ternary cements. *Cement and Concrete Composites*. 33(1): p. 30-38.

Ye, G. et al. (2007) Influence of limestone powder used as filler in SCC on hydration and microstructure of cement pastes. *Cement and Concrete Composites*. 29(2): p. 94-102.

Péra, J., Husson S., and Guilhot B. (1999) Influence of finely ground limestone on cement hydration. *Cement and Concrete Composites*. 21(2): p. 99-105.

Groot C (1993) Effects of water on mortar brick bond. University of Delft, The Netherlands

Aly, M and Pavía S. (2016) Effect of limestone aggregate on the properties of natural hydraulic lime mortar (NHL 5). Rehabend

Pavía S. and Aly M. (2016) Influence of aggregate and supplementary cementitious materials on the properties of hydrated lime (CL90s) mortars. *Materiales de Construcción. In press.*

Bonavetti, V.L., V.F. Rahhal, and E.F. Irassar (2001) Studies on the carboaluminate formation in limestone filler-blended cements. *Cement and Concrete Research*. 31(6): p. 853-859.

Menéndez, G., V. Bonavetti, and E.F. Irassar (2003) Strength development of ternary blended cement with limestone filler and blast-furnace slag. *Cement and Concrete Composites*. 25(1): p. 61-67.

Scannell S., Lawrence M. and Walker P. (2014) Impact of aggregate type on air lime mortar properties. *Energy Procedia* 62 81 – 90